Am J Transl Res 2022;14(10):6906-6923
www.ajtr.org /ISSN:1943-8141/AJTR0143110

Original Article

Identification of biomarkers and key pathways in synovial sarcoma cells exposed to anlotinib by integrating bioinformatics analysis and experimental validation

Xiaoli Liu[1], Mengqi Fu[2], Changji Jia[2], Xiaoying Wang[3], Yan Song[4*], Changliang Peng[2*]

Departments of [1]Hematology, [2]Spinal Surgery, [3]Pathology, [4]Nephrology, The Second Hospital of Shandong University, Jinan 250033, Shandong, China. [*]Equal contributors.

Received March 25, 2022; Accepted August 20, 2022; Epub October 15, 2022; Published October 30, 2022

Abstract: Objective: To identify potential biomarkers, key pathways and modules following the exposure of synovial sarcoma (SS) cells to anlotinib. Methods: In the current study, we integrated multiple bioinformatics methods to identify the hub genes and key pathways associated with the effects of anlotinib treatment in SS cells. In addition, we used reverse transcription-quantitative real-time polymerase chain reaction (RT-qPCR) to validate the expression levels of the identified hub genes in SS cells treated with anlotinib. Results: In total, 183 differentially expressed genes (DEGs) were identified, of which 47 were upregulated and 136 were downregulated. Gene Ontology (GO) and Kyoto Encyclopedia of Genes and Genomes (KEGG) pathway analyses showed that the DEGs were predominantly involved in cell division and cell cycle progression. A total of two modules were identified from the protein-protein interaction network using the MCODE plugin in Cytoscape, where module 1 was the most significant. By combining the results of CytoHubba analysis based on the module 1 and The Cancer Genome Atlas database, six real hub genes, *cyclin* (*CCN*) *A2, kinesin family member 2C, cell division cycle 20, CCNB2, aurora kinase B* and *CCNB1*, were identified. Subsequent GO and KEGG pathway analysis revealed that these six real hub genes were significantly associated with the cell cycle and mitosis. Finally, RT-qPCR verified that the mRNA expression levels of these six real hub genes were significantly decreased in SS cells treated with anlotinib compared with those in the control group. Altogether, our study identified biomarkers and key pathways associated with the effects of anlotinib treatment in SS cells, which may provide novel insights into the underlying mechanism of anlotinib treatment in SS.

Keywords: Synovial sarcoma, anlotinib, bioinformatic analysis, differentially expressed genes, hub genes, pathway

Introduction

Synovial sarcoma (SS) is a high-grade, malignant soft-tissue sarcoma (STS) and has a 5-year survival rate of <66% [1]. Currently, the main treatment method for localized SS is radical surgery combined with neoadjuvant chemotherapy and/or radiotherapy [2]. According to recently published National Comprehensive Cancer Network (NCCN) and European Society of Medical Oncology (ESMO) guidelines, adjuvant chemotherapy is recommended in high-risk localized STS patients [3, 4]. However, patients with SS typically have a high possibility of recurrence and metastasis after early operation [5]. In addition, patients frequently become desensitized and unresponsive to chemotherapy and radiotherapy [6]. Therefore, it remains in demand to discover novel effective therapeutic targets for SS.

Receptor tyrosine kinases (RTKs) have been previously reported to regulate tumor proliferation, growth, angiogenesis and metastasis, thereby serving important roles in tumor progression [7, 8]. Therefore, targeting RTKs may be an effective strategy for clinical treatment of a variety of solid tumors including renal cell carcinoma [9], lung cancer [10], hepatocellular carcinoma [11], etc. Anlotinib is a novel multi-target RTK inhibitor that has been reported to effectively exert anti-tumor activity in patients

with advanced refractory solid tumors [12]. It can mainly target vascular endothelial growth factor receptor (VEGFR), fibroblast growth factor receptor (FGFR), platelet-derived growth factor receptors (PDGFR) and c-kit [13]. Previously, it has been shown that anlotinib is safe and highly effective for the treatment of various solid tumors, including lung cancer [14], esophageal squamous cell carcinoma [15], STS [16, 17], etc. In addition, a previous study investigated the potential anti-tumor effects of anlotinib in SS [18], which demonstrated that the anti-tumor properties of anlotinib is mediated through the downregulation of GINS complex subunit 1 expression downstream. However, the differentially expressed genes (DEGs) between the control and anlotinib-treated SS cells were not investigated using an integrated bioinformatics analysis. More importantly, the potential biomarkers and key pathways that may be involved in the biological process of anlotinib-treated SS cells were not explored.

In the present study, we identified the DEGs from the GSE109468 dataset [18] between the control and anlotinib-treated SS cells. Next, Gene Ontology (GO) and Kyoto Encyclopedia of Genes and Genomes (KEGG) pathway enrichment analysis were applied to explore the functions of the identified DEGs. Furthermore, protein-protein interaction (PPI) network and module analysis of the DEGs were performed to identify possible biomarkers and key pathways associated with the biological processes that occur after anlotinib treatment in SS. Subsequently, using The Cancer Genome Atlas (TCGA) database, the expression levels of the identified hub genes between normal and SS samples were assessed. GO and KEGG pathway enrichment analyses of the identified real hub genes were then performed using the WEB-based GEne SeT AnaLysis Toolkit (WebGestalt) database. Finally, the mRNA expression levels of the identified hub genes in the SS cell lines treated with anlotinib were verified by reverse transcription-quantitative real-time polymerase chain reaction (RT-qPCR). In conclusion, this study identified six real hub genes, namely *cyclin (CCN) A2, kinesin family member (KIF) 2C, cell division cycle (CDC) 20, CCNB2, aurora kinase B (AURKB)* and *CCNB1*. These hub genes were significantly enriched in cell cycle progression and mitosis, which may provide potential biomarkers and targets to improve the clinical efficacy of anlotinib treatment in patients with SS.

Materials and methods

Data collection

The microarray dataset of GSE109468 [18] were obtained from the Gene Expression Omnibus database (GEO; https://www.ncbi.nlm.nih.gov/geo/). The GSE109468 dataset based on the GPL15207 platform (Affymetrix Human Gene Expression Array) included three groups of human synovial sarcoma (SW982) cells treated with anlotinib and three groups of SW982 cells treated without anlotinib. In addition, the RNA-seq expression data of nine human SS tumor tissues and two normal tissues were obtained from TCGA database (https://portal.gdc.cancer.gov/) to further investigate the results.

DEGs analysis

The DEGs between control and anlotinib-treated SS cells were screened using GEO2R (https://www.ncbi.nlm.nih.gov/geo/geo2r/), which allows for the comparison of different gene expression data among ≥ two groups of samples. The DEGs were identified according to the following criteria: Adjusted *P*-value <0.05 and $|\log_2$ fold change (FC)| ≥1.0. Heatmaps of the DEGs were generated using the Heml software (Version 1.0.3.7; http://hemi.biocuckoo.org/faq.php) [19], a toolkit for illustrating heatmaps.

GO and KEGG pathway analysis

We used the Database for Annotation, Visualization and Integrated Discovery (DAVID) database (Version 6.8; https://david.ncifcrf.gov/) to perform GO and KEGG pathway enrichment analysis of the DEGs, and P<0.05 was used as the cut-off criterion. GO terms enrichment analysis was classified into three major groups, specifically biological process (BP), cellular component (CC) and molecular function (MF).

Gene set enrichment analysis (GSEA)

To estimate whether a predefined list of genes display statistical significance between two

phenotypes [20], GSEA was conducted between control and anlotinib-treated SS cells using the GSEA software (Version 4.2.3; https://www.gsea-msigdb.org/gsea/index.jsp). The number and type of permutations was defined as '1,000' and 'phenotype', respectively. The metric used for ranking genes was set as 'Signal2Noise'. The minimum and maximum sizes of the selected gene sets were 15 and 500, respectively. Subsequently, the 'h.all.v7.1.symbols.gmt (Hallmarks)' and 'c5.all.v7.1.symbols.gmt (Gene ontology)' downloaded from the Molecular Signatures Database (MSigDB; http://software.broadinstitute.org/gsea/msigdb/index.jsp) were chosen to be the reference gene sets for performing the GSEA assay. The cut-off criteria were set as nominal P<0.05, false discovery rate (FDR) q-value <0.25 and enrichment score >0.6.

PPI network construction and module analysis

We used the Search Tool for the Retrieval of Interacting Genes (STRING) database (version 11.5, https://string-db.org) for exploring the PPI network of DEGs, where the combined score >0.4 was set as the cut-off criterion. The Cytoscape software (version 3.8.0, https://cytoscape.org) was then used to visualize and analyze the PPI network. Subsequently, the Molecular Complex Detection (MCODE, version 1.5.1) plugin of Cytoscape software was used to screen the significant modules of the PPI network with the following parameters: MCODE scores >5; degree cut-off =2; node score cut-off =0.2; k-core =2; and max. depth =100 [21]. GO and KEGG pathway analyses were also performed in the modules using the STRING database, where differences were considered to be statistically significant with FDR<0.05.

Hub genes identification and analysis

The hub genes were identified using CytoHubba (version 0.1), which is a novel plugin for Cytoscape that can identify hub objects and sub-networks from complex interactomes [22]. For identifying network hub genes, a total of 11 topological algorithms are provided by CytoHubba. Among all the algorithms, Maximal Clique Centrality (MCC) tended to perform better compared with others in predicting PPI network hub genes [22]. Therefore, for the present study, the MCC algorithm was used to identify the hub genes [22]. Subsequently, GO analysis of the identified hub genes was analyzed using the Biological Networks Gene Oncology tool (BiNGO; Version 3.0.3) plugin of Cytoscape [23] with a threshold FDR value <0.05.

The expression levels of the identified hub genes were then validated in TCGA database. A total of 11 samples were chosen for gene expression level analysis, including nine SS tissues and two normal tissues. Unpaired t-test was conducted to evaluate the statistical significance, where the level of significance was defined at P<0.05. Finally, the aforementioned validated hub genes were analyzed using the WebGestalt database (http://www.webgestalt.org/) [24] with a threshold of FDR<0.05 to perform the GO and KEGG pathway enrichment analysis.

Cell lines and cell culture

Human SS cell lines SW982 and HS-SY-II were kindly provided by Peking University People's Hospital (Beijing, China). SW982 and HS-SY-II cells were grown in Dulbecco's modified Eagle's medium (Gibco; Waltham, USA), containing 10% fetal bovine serum (Gibco; Waltham, USA) in a humidified atmosphere under 5% CO_2 at 37°C. The two cell lines were incubated with anlotinib (Selleck; Houston, USA) at an indicated condition as previously described [18].

RT-qPCR

According to the manufacturer's protocol, the total RNAs from SW982 and HS-SY-II cells were isolated using RNA-easy Isolation Reagent (cat. no. R701-01; Vazyme; Nanjing, China). Next, the complementary DNA (cDNA) was synthesized from the total RNAs using HiScript® II 1st Strand cDNA Synthesis Kit (+gDNA wiper; cat. no. R212-01; Vazyme; Nanjing, China). qPCR was performed in an Applied Biosystems System using ChamQ SYBR Color qPCR Master Mix (Without ROX; cat. no. Q421-02; Vazyme; Nanjing, China). The thermocycling conditions were as follows: Pre-denaturation for 30 sec at 95°C, followed by 40 cycles of 95°C for 10 sec and 60°C for 30 sec. A melting curve was analyzed for each reaction from 60 to 95°C. mRNA expression levels were calculated using the $2^{-\Delta\Delta Cq}$ method [25], where the expression val-

Table 1. Identification of DEGs associated with anlotinib treatment of SS cells

Regulation	Genes
Upregulated (n=47)	*SLC7A11, MMP3, IL24, GDF15, LOC100129518, IL6, SLC16A6, NUPR1, SERPINB2, SPP1, IL1A, IFI44L, GPNMB, CCL20, KYNU, DDIT3, FYB, RND3, FTH1, MME, CSTA, FOLR3, SQSTM1, IL1B, HMOX1, NOV, CXCL2, EREG, TM4SF19, EPGN, C3, CARD16, FCMR, RRAGD, SPINK1, LCP1, ZNF655, CHI3L1, CSF2, CLCA2, RAB27B, PVRL4, SPX, WISP2, BEX2, SOD2, TM4SF19-TCTEX1D26*
Downregulated (n=136)	*GINS2, CCL2, CDCA7, CDC20, E2F8, MGP, NEURL1B, HCG22, UBE2C, MCM7, RRM2, LMNB1, PRC1, ZWINT, NUSAP1, CENPA, KIF2C, BIRC5, PHF19, KIF20A, MCM2, PBK, SERTAD4, GINS4, TACC3, SPC25, TK1, FEN1, TOP2A, H2AFX, KIF22, ASF1B, CDC25C, CDCA8, NCAPG2, CCNF, CKS1B, CDCA5, AURKB, ANLN, MTFR2, UHRF1, APOBEC3B, BUB1, CDC6, HMGB3, CCNB2, LYPD1, FAM83D, CDC45, BUB1B, PRR11, HIST1H4C, FANCI, CCNA2, CDK1, POLE2, GTSE1, MCM3, FKBP5, RNASEH2A, CDCA2, SPAG5, BLM, APOBEC3A, DPYSL3, FAM72A, SHCBP1, NEK2, GINS1, KIAA0101, FAM64A, RACGAP1, PMEPA1, NUF2, CCNB1, DEPDC1B, FOXM1, VCAN, ESCO2, DTL, HJURP, TMPO, CDCA3, MND1, PLK4, ARHGAP11A, TNFRSF19, MKI67, ERCC6L, NCAPG, SPC24, TROAP, TCF19, CIT, BARD1, FBXO5, NCAPH, KIF15, RTKN2, CLSPN, FANCD2, ORC6, CDKN2C, CCDC34, NCAPD3, FAM111B, MCM10, ZNF367, LMNB1, CDC7, PAQR4, DLEU2, DSCC1, KIF14, FANCD2, LIN9, HAUS8, PSMC3IP, HELLS, DLEU2, KLHL23, ACBD7, RNF150, TCF19, APOBEC3A_B, APOBEC3B, FAM72B, FAM72C, FAM72D, ARHGAP11B, LOC100288637, PCIF1, FANCD2P2, DLEU2L, PHOSPHO2-KLHL23*

ues were normalized to those of β-actin. All primer sequences used for RT-qPCR were listed in Table S1.

Statistical analysis

For RT-qPCR, all the experiments were conducted in triplicate. The data were shown as the mean ± standard deviation. Statistical analysis was performed using the GraphPad Prism software (version 8.0; Graphpad; San Diego, USA). Differences between two groups were assessed using paired Student's t-test. $P<0.05$ was considered to indicate a statistically significant difference.

Results

Identification of DEGs

A total of 183 DEGs that met the cut-off criteria were identified from GSE109468, including 47 upregulated and 136 downregulated genes (**Table 1**; **Figure 1A**). Heatmap analysis revealed that these genes displayed differential expression profiles between anlotinib-treated SS cells and untreated SS cells (**Figure 1B**).

Functional enrichment analysis

In terms of BP, the 183 DEGs were mainly enriched in 'cell division', 'mitotic nuclear division', 'DNA replication', 'sister chromatid cohesion' and 'DNA replication initiation' (**Figure 2A**). For CC analysis, the 183 DEGs were particularly enriched in 'nucleoplasm', 'condensed chromosome kinetochore', 'chromosome, centromeric region', 'nucleus' and 'midbody' (**Figure 2B**). In terms of MF, the 183 DEGs were mostly involved in 'protein binding', '3'-5' DNA helicase activity', 'DNA replication origin binding', 'protein kinase binding' and 'deoxycytidine deaminase activity' (**Figure 2C**). For KEGG pathway analysis, the 183 DEGs were highly associated with 'cell cycle', 'DNA replication', 'rheumatoid arthritis', 'TNF signaling pathway' and 'oocyte meiosis' (**Figure 2D**).

GSEA

To identify the molecular mechanisms of the DEGs between control and anlotinib-treated SS cells, GSEA of hallmark gene sets was performed and the results revealed that 19/50 gene sets were downregulated in anlotinib-treated group, where 15 gene sets were significant at FDR<25% and 14 gene sets were significantly enriched at nominal $P<0.05$. The top three downregulated gene sets were E2 transcription factor targets, G_2/M checkpoint and mitotic spindle (**Figure 3A**). According to the GO gene sets, 2,423/5,372 gene sets are downregulated in anlotinib-treated group, 1,043 gene sets are significantly enriched at FDR<25% and 1,083 gene sets are significantly enriched at nominal $P<0.05$. The top five enriched GO

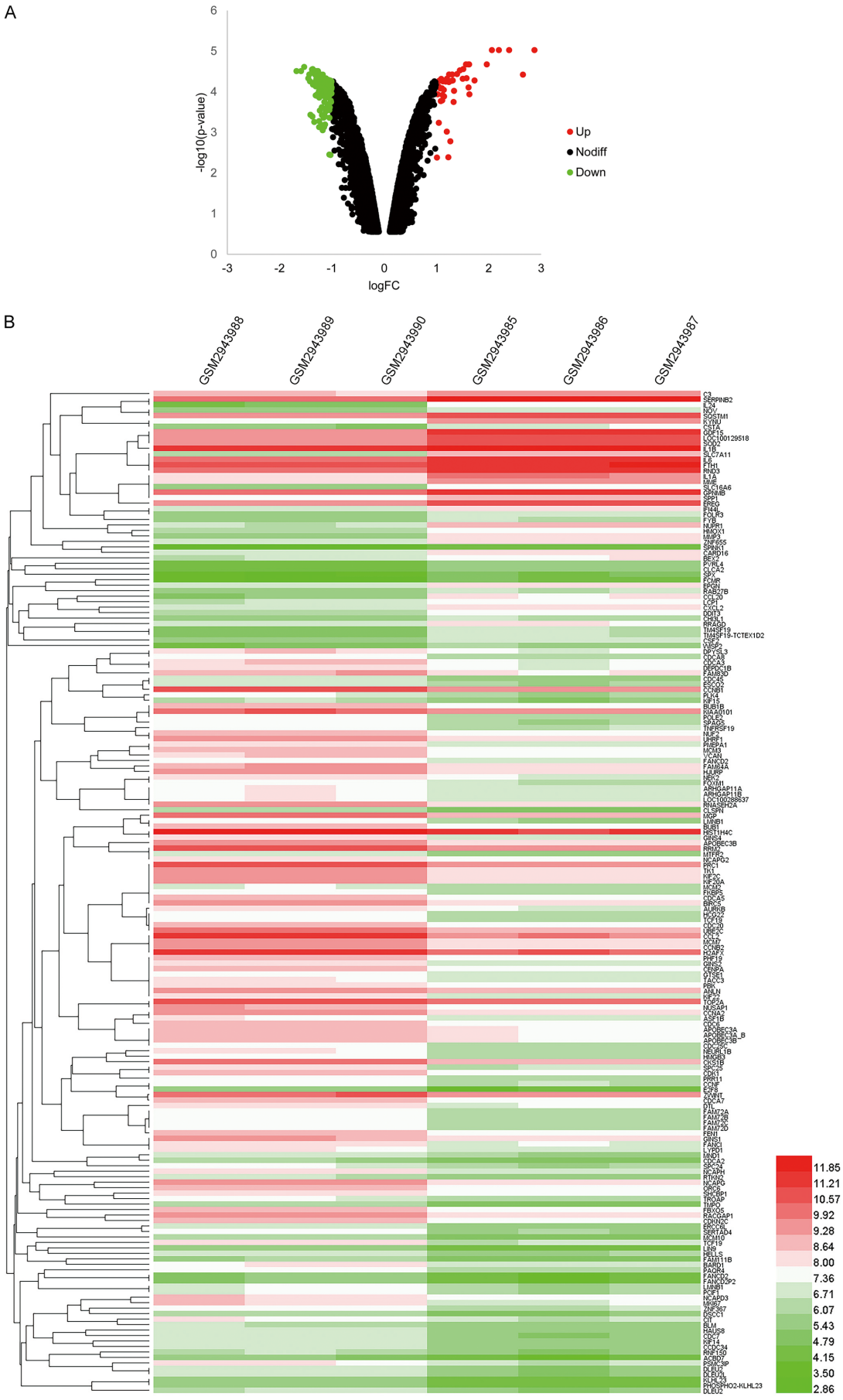
A
-log10(p-value)
logFC
Up
Nodiff
Down
B
GSM2943988
GSM2943989
GSM2943990
GSM2943985
GSM2943986
GSM2943987
11.85
11.21
10.57
9.92
9.28
8.64
8.00
7.36
6.71
6.07
5.43
4.79
4.15
3.50
2.86

Figure 1. Identification of the DEGs after anlotinib treatment in SS cells. A. Volcano plot of DEGs for the GSE109468 dataset. Red represented upregulated DEGs, green represented downregulated DEGs and black represented non-differentially expressed genes. Genes with adjusted *P*-value <0.05 and $|\log_2$ fold change$| \geq 1.0$ are considered to be DEGs. B. Heatmap of the 183 DEGs identified between control and anlotinib-treated SS cells. GSM2943988, GSM2943989 and GSM2943990 represented the negative control group, while GSM2943985, GSM2943986 and GSM2943987 represented the anlotinib treatment group. SS, synovial sarcoma; DEGs, differentially expressed genes; up, upregulated; down, downregulated; Nodiff, non-differentially expressed genes.

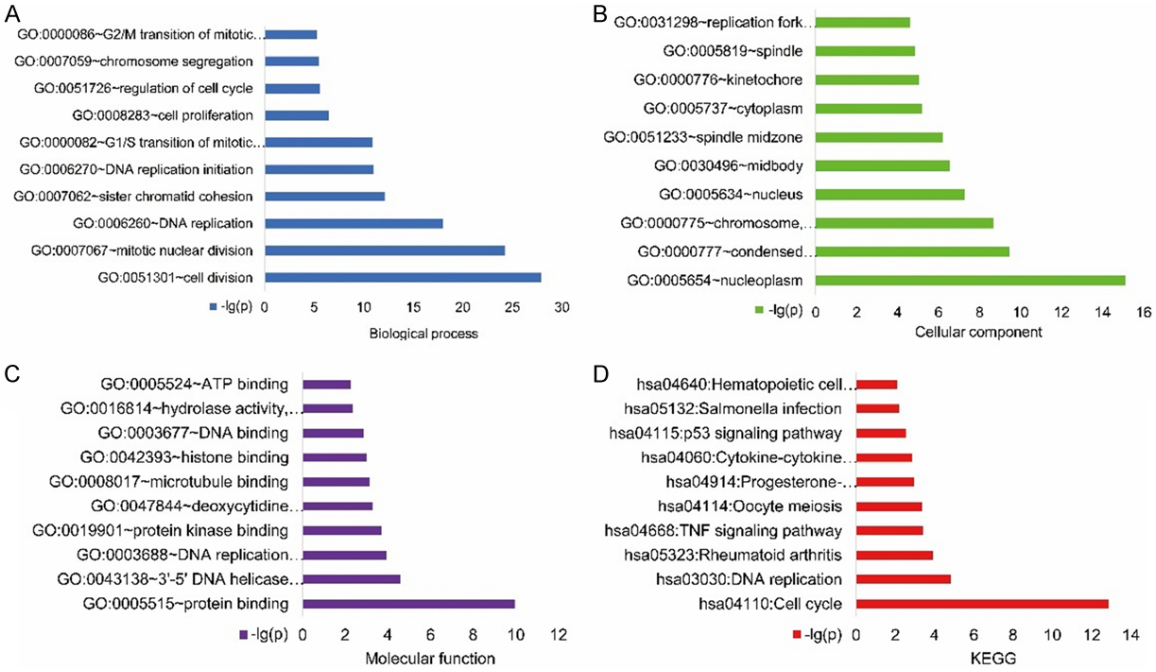

Figure 2. GO and KEGG pathway enrichment analysis of DEGs using the Database for Annotation, Visualization and Integrated Discovery database. A. Top 10 significant terms according to the GO biological process enrichment analysis of DEGs. B. Top 10 significant terms according to the GO cellular component enrichment analysis of DEGs. C. Top 10 significant terms according to the GO molecular function enrichment analysis of DEGs. D. Top 10 significant terms according to the KEGG pathway enrichment analysis of DEGs. GO, gene ontology; KEGG, Kyoto Encyclopedia of Genes and Genomes; DEGs, differentially expressed genes.

terms of the DEGs associated with anlotinib treatment were 'basic helix-loop-helix transcription factor binding', 'ventricular cardiac muscle cell differentiation', 'regulation of meiotic cell cycle', 'atrial septum morphogenesis' and 'cleavage furrow' (**Figure 3B**).

PPI network and modular analysis

To explore the interaction of the screened 183 DEGs, the STRING database was used to construct the PPI network. The results revealed that a relevant PPI network was successfully constructed, which contained 175 nodes and 3,550 edges (**Figure 4A**). This PPI network of the DEGs was then visualized using the Cytoscape software (**Figure 4B**). Based on the entire network, the Module analysis was then performed using the MCODE plugin of Cytoscape. The results showed that two significant modules with a score ≥5 were identified from the network. There were 75 nodes and 2,422 edges in Module 1 (**Figure 4C**), whereas a total of 8 nodes and 28 edges were detected in Module 2 (**Figure 4D**). Furthermore, functional analysis of the genes involved in the two modules was performed using the STRING database. The results revealed that genes in module 1 were mainly enriched in 'cell cycle' for BP, 'DNA replication origin binding' for MF, 'chromosome region' for CC and 'cell cycle' for KEGG (**Table 2**). The genes in module 2 were mainly associated with 'cytokine-mediated signaling pathway' for BP, 'cytokine activity' for MF, 'extracellular space' for CC and rheumatoid arthritis for KEGG (**Table 3**). Module 1 was the

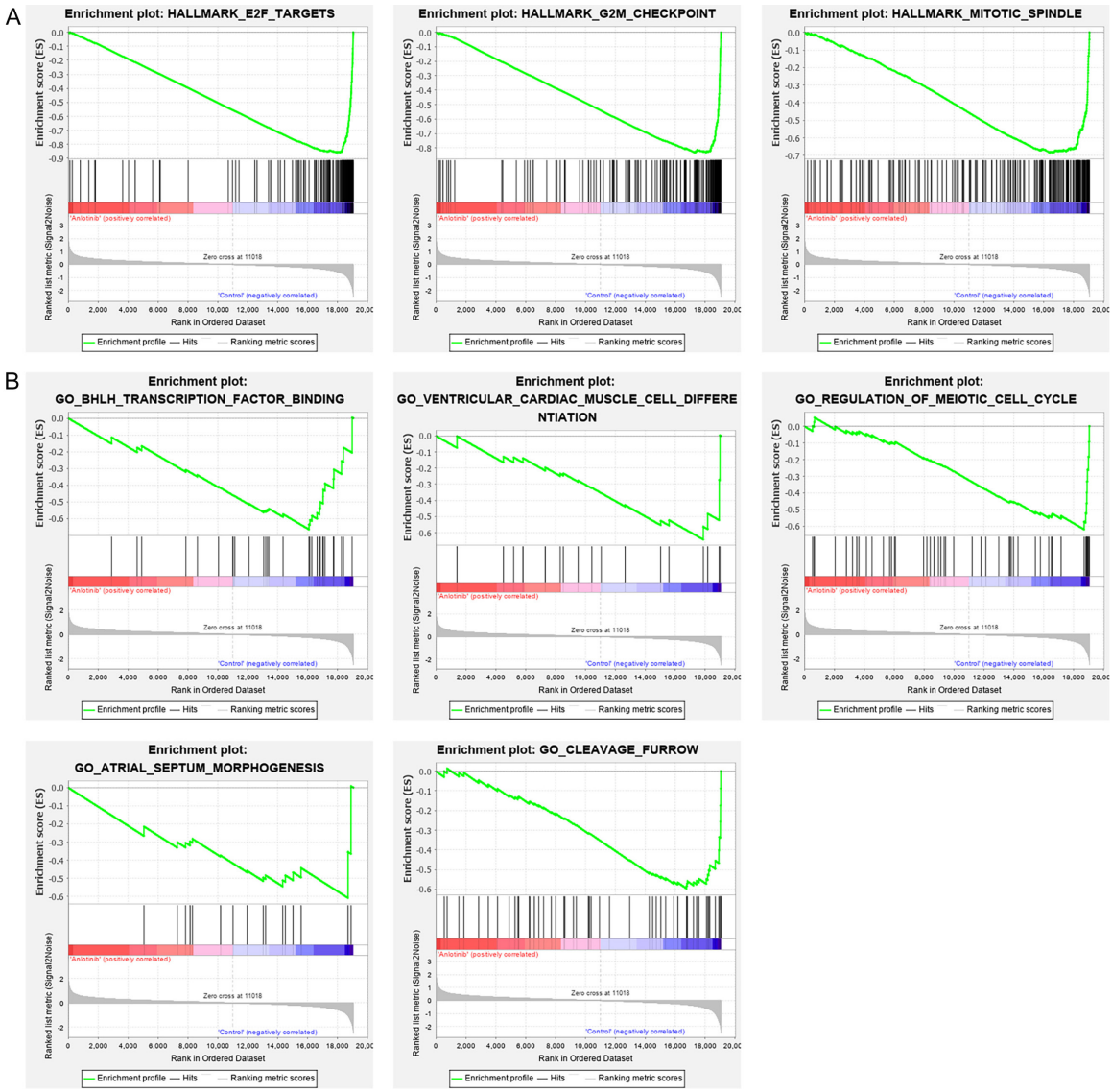

Figure 3. GSEA results. A. The top three representative functional gene sets of GSEA according to the hallmark gene sets. GSEA hallmark term analysis showed that E2 transcription factor targets, G_2/M checkpoint and mitotic spindle are significantly enriched processes associated with anlotinib treatment. B. The top five representative functional gene sets of GSEA based on the GO gene sets. GSEA revealed that enrichment of the five most significant GO terms are 'basic helix-loop-helix transcription factor binding', 'ventricular cardiac muscle cell differentiation', 'regulation of meiotic cell cycle', 'atrial septum morphogenesis' and 'cleavage furrow', which are associated with anlotinib treatment. GSEA, Gene set enrichment analysis; GO, gene ontology.

most significant of the two modules identified by MCODE analysis.

Hub genes identification, validation, and analysis

The connectivity degree of each node in PPI in the two modules was calculated using CytoHubba according to the MCC algorithm. Finally, the top 10 hub genes, *CCNA2, ribonucleotide reductase regulatory subunit 2 (RRM2), KIF2C, CDC20, CCNB2, budding uninhibited by benzimidazoles (BUB) 1, BUB1B, AURKB, CCNB1* and *KIF20A*, were identified in module 1 (**Table 4**; **Figure 5A**). In addition, *C-X-C motif chemokine ligand 2, C-C motif chemokine ligand (CCL) 20, colony-stimulating factor 2, interleukin (IL) 6, matrix metalloproteinase 3, CCL2, IL1B* and *IL1A* were among hub genes in module 2 (**Table 5**; **Figure 4D**). Subsequently, the hub genes in module 1 were subjected to BP analysis using the BiNGO

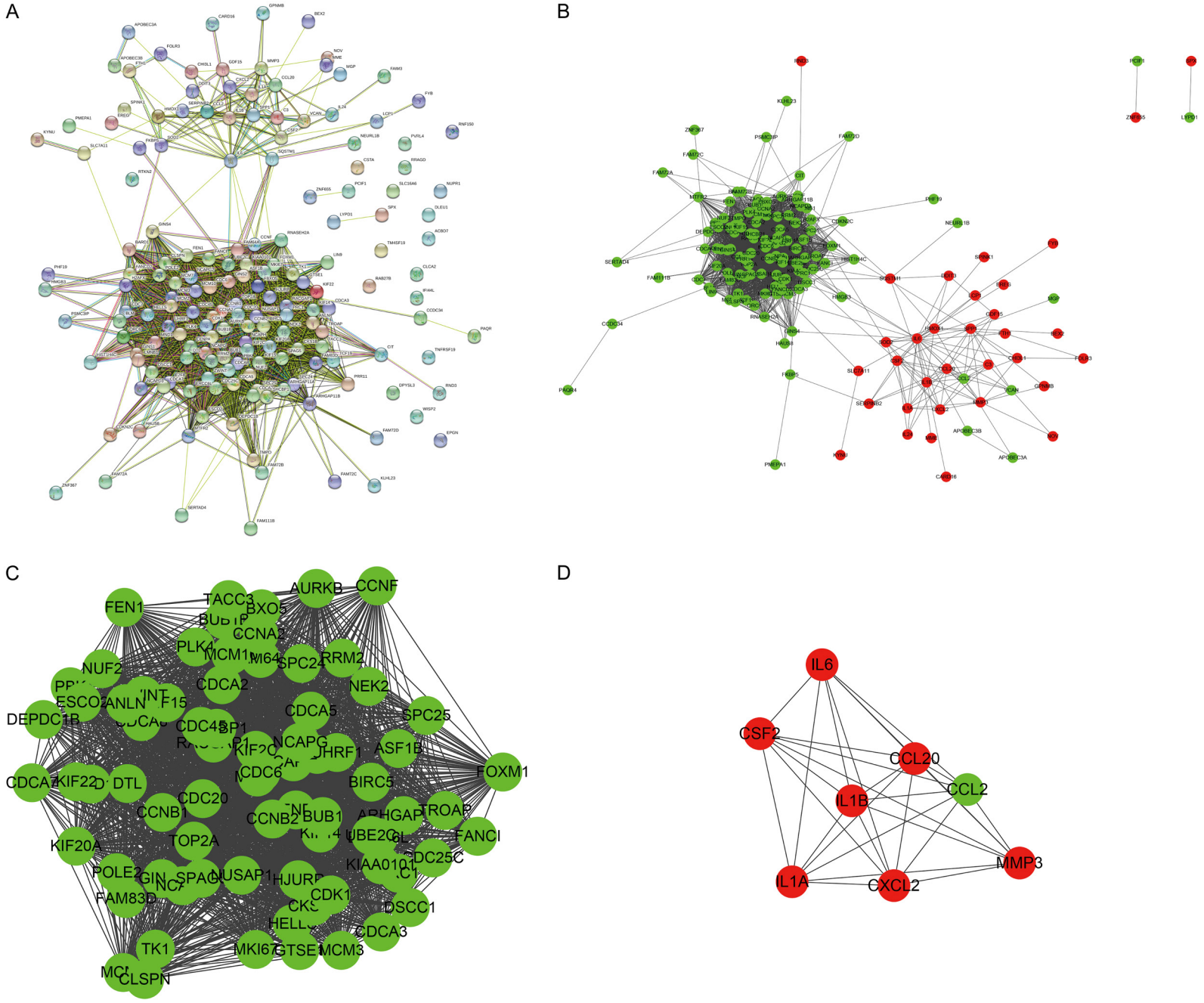
A
B
C
D
AURKB
CCNF
FEN1
TACC3
BUB1B
CCNA2
PLK1
MCM10
NUF2
CDCA2
NEK2
CDCA5
SPC25
DEPDC1B
CDC45
NCAPG
KIF2C
ASF1B
FOXM1
CDCA8
KIF22
DTL
BIRC5
CDC20
CCNB1
CCNB2
BUB1
TROAP
KIF20A
TOP2A
FANCI
CDC25C
KIAA0101
POLE2
RAD54L
USP1
CDK1
FAM83D
DSCC1
CDCA3
TK1
MKI67
GTSE1
MCM3
CLSPN
IL6
CSF2
CCL20
CCL2
IL1B
MMP3
IL1A
CXCL2

Figure 4. PPI network and modular analysis. A. PPI of DEGs were analyzed using the Search Tool for the Retrieval of Interacting Genes database. B. The PPI network of DEGs was established using the Cytoscape software. Red nodes indicated upregulated genes, whereas green nodes represented downregulated genes. C. The most significant module 1 was identified from the PPI network using the Molecular Complex Detection plugin of Cytoscape. Green nodes represented downregulated genes. D. The Module 2 was identified from the PPI network. Red and green nodes represented upregulated and downregulated genes, respectively. PPI, protein-protein interaction; DEGs, differentially expressed genes.

Table 2. The top 3 enriched GO terms and KEGG pathways of the genes in the module 1

Category	Term ID	Term description	Count	FDR
BP	GO:0007049	Cell cycle	66	1.46E-62
BP	GO:0000278	Mitotic cell cycle	51	4.75E-51
BP	GO:1903047	Mitotic cell cycle process	49	2.98E-50
MF	GO:0003688	DNA replication origin binding	6	3.63E-06
MF	GO:0008017	Microtubule binding	11	9.11E-06
MF	GO:0005524	ATP binding	22	2.08E-05
CC	GO:0098687	Chromosome region	27	2.11E-25
CC	GO:0005694	Chromosome	44	2.67E-24
CC	GO:0000775	Chromosome, centromeric region	22	4.31E-23
KEGG	hsa04110	Cell cycle	12	3.13E-11
KEGG	hsa04914	Progesterone-mediated oocyte maturation	7	1.93E-05
KEGG	hsa03030	DNA replication	7	5.35E-05

Table 3. The top 3 enriched GO terms and KEGG pathways of the genes in the module 2

Category	Term ID	Term description	Count	FDR
BP	GO:0019221	Cytokine-mediated signaling pathway	8	2.81E-08
BP	GO:0071222	Cellular response to lipopolysaccharide	6	1.41E-07
BP	GO:0009617	Response to bacterium	7	5.58E-07
MF	GO:0005125	Cytokine activity	7	9.78E-10
MF	GO:0005126	Cytokine receptor binding	7	1.16E-09
MF	GO:0070851	Growth factor receptor binding	4	9.17E-05
CC	GO:0005615	Extracellular space	8	0.00087
KEGG	hsa05323	Rheumatoid arthritis	8	6.41E-17
KEGG	hsa04657	IL-17 signaling pathway	7	9.13E-14
KEGG	hsa04668	TNF signaling pathway	7	2.29E-13

Table 4. Hub genes identified in the key module 1

Genes	Description	MCODE Score	adj.*P*.Value	Log FC
CCNA2	Cyclin A2	46.9	6.40E-05	-1.0960
AURKB	Aurora Kinase B	46.9	5.53E-05	-1.13896
RRM2	Ribonucleotide Reductase Regulatory Subunit M2	46.9	3.07E-05	-1.28315
KIF2C	Kinesin Family Member 2C	46.9	3.78E-05	-1.20639
CCNB1	Cyclin B1	46.9	9.92E-05	-1.08588
BUB1	BUB1 Mitotic Checkpoint Serine/Threonine Kinase	46.9	5.55E-05	-1.15767
KIF20A	Kinesin Family Member 20A	46.9	3.78E-05	-1.18615
BUB1B	BUB1 Mitotic Checkpoint Serine/Threonine Kinase B	46.9	6.07E-05	-1.19207
CDC20	Cell Division Cycle 20	46.9	3.07E-05	-1.37731
CCNB2	Cyclin B2	46.9	5.88E-05	-1.03654

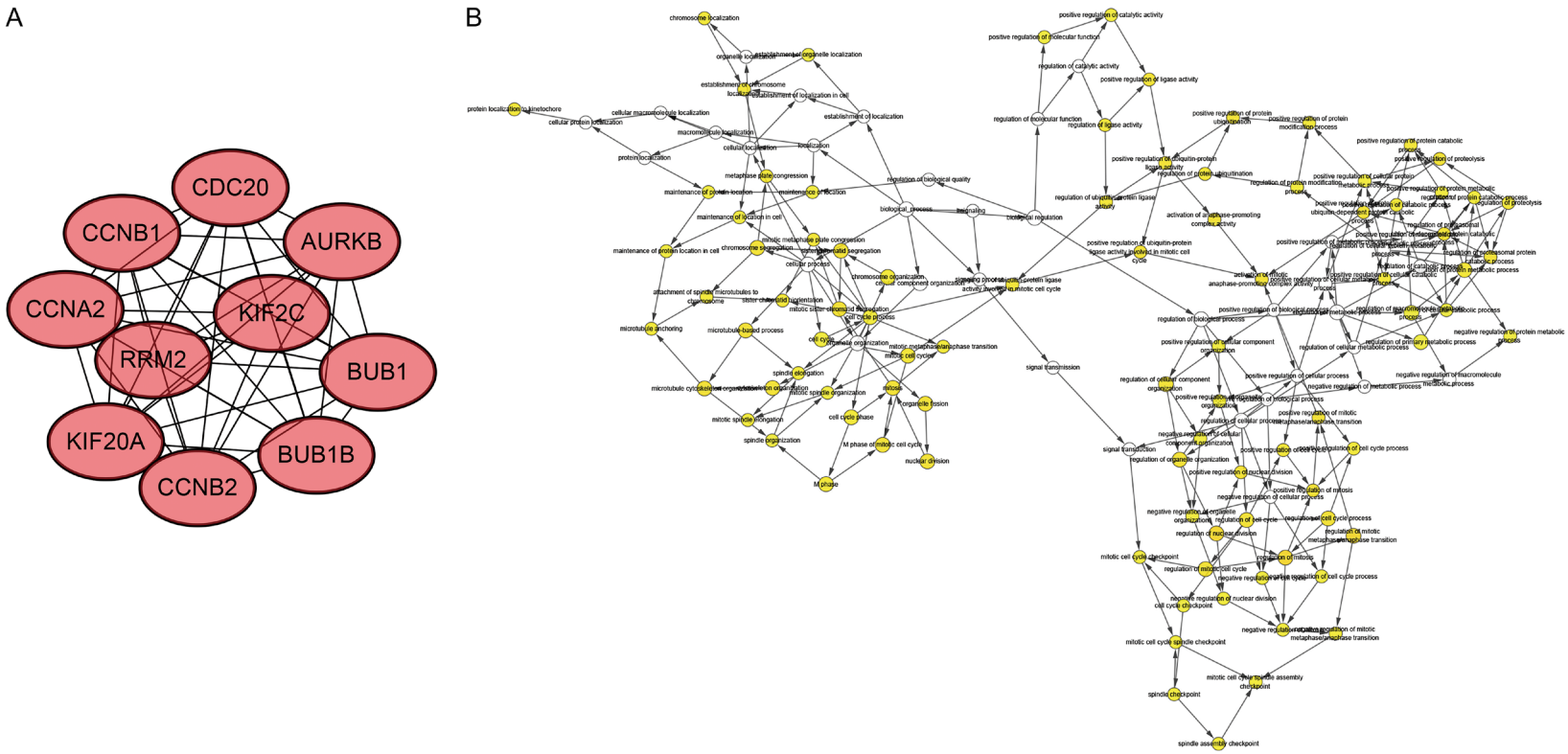

Figure 5. Identification of hub genes and biological process analysis of the hub genes. A. The top 10 hub genes were identified from module 1 using Maximal Clique Centrality algorithm analysis. B. Biological process analysis of hub genes was performed using the Biological Networks Gene Oncology tool. The color depth of nodes was filled in accordance with the FDR values. FDR<0.05 was considered to indicate a statistically significant difference. FDR, false discovery rate.

Table 5. Hub genes identified in the key module 2

Genes	Description	MCODE Score	adj.*P*.Value	logFC
IL1A	Interleukin 1 Alpha	7	3.65E-05	1.390683
CXCL2	C-X-C Motif Chemokine Ligand 2	7	5.76E-05	1.237424
CSF2	Colony Stimulating Factor 2	7	1.70E-04	1.080502
CCL20	C-C Motif Chemokine Ligand 20	7	3.78E-05	2.65226
MMP3	Matrix Metallopeptidase 3	7	9.41E-06	2.387417
IL6	Interleukin 6	7	2.11E-05	1.610271
CCL2	C-C Motif Chemokine Ligand 2	7	2.75E-05	-1.36825
IL1B	Interleukin 1 Beta	7	5.35E-05	1.0527

Table 6. The BiNGO results of the 10 hub genes in the module 1

GO ID	Description	FDR	Genes
30071	regulation of mitotic metaphase/anaphase transition	1.49E-03	*CDC20; BUB1*
51783	regulation of nuclear division	1.49E-03	*CDC20; BUB1*
7088	regulation of mitosis	1.49E-03	*CDC20; BUB1*
70	mitotic sister chromatid segregation	5.42E-03	*CDC20; BUB1*
7346	regulation of mitotic cell cycle	5.42E-03	*CDC20; BUB1*
819	sister chromatid segregation	5.42E-03	*CDC20; BUB1*
10564	regulation of cell cycle process	5.42E-03	*CDC20; BUB1*
226	microtubule cytoskeleton organization	5.42E-03	*CDC20; BUB1*
7017	microtubule-based process	5.48E-03	*CDC20; BUB1*
33043	regulation of organelle organization	5.48E-03	*CDC20; BUB1*

Cytoscape plugin, where the results revealed that majority of the hub genes were significantly enriched in 'regulation of mitotic metaphase/anaphase transition', 'regulation of nuclear division' and 'regulation of mitosis' (**Table 6**; **Figure 5B**).

TCGA dataset was then used to validate the expression status of the 10 hub genes *CCNA2, RRM2, KIF2C, CDC20, CCNB2, BUB1, BUB1B, AURKB, CCNB1* and *KIF20A*. We found that the expression levels of *CCNA2, KIF2C, CDC20, CCNB2, AURKB* and *CCNB1* were significantly higher in SS tissues compared with those in the normal tissues, whilst those of *RRM2, KIF20A, BUB1* and *BUB1B* exhibited no significant differences in their expression levels (**Figure 6**). Therefore, *CCNA2, KIF2C, CDC20, CCNB2, AURKB* and *CCNB1* were confirmed to be the real hub genes that are the most likely to be associated with anlotinib treatment.

The WebGestalt online tool was then used to further explore the GO and KEGG pathway enrichment of these six real hub genes. The results revealed that these six real hub genes were significantly associated with 'regulation of chromosome segregation', 'regulation of mitotic nuclear division', 'mitotic sister chromatid segregation', 'regulation of nuclear division' and 'mitotic nuclear division' for BP (**Figure 7A**; Table S2). For CC, enrichments were found for 'cyclin-dependent protein kinase holoenzyme complex', 'serine/threonine protein kinase complex', 'protein kinase complex', 'condensed chromosome, centromeric region' and 'kinetochore' (**Figure 7B**; Table S3). For MF, enrichments for 'histone kinase activity', 'cyclin-dependent protein kinase activity', 'cyclin-dependent protein serine/threonine kinase regulator activity', 'cyclin-dependent protein serine/threonine kinase activity' and 'protein kinase regulator activity' were found (**Figure 7C**; Table S4). In terms of KEGG pathways, the six real hub genes were significantly enriched in 'cell cycle', 'progesterone-mediated oocyte maturation', 'p53 signaling pathway', 'oocyte meiosis' and 'cellular senescence' (**Figure 7D**; Table S5). Consistent with the data of the aforementioned DAVID and BiNGO analysis, it is shown that these six real hub genes (*CCNA2, KIF2C, CDC20, CCNB2, AURKB* and *CCNB1*) were mainly associated with cell cycle and mitosis. Therefore, it is likely that the anti-tumor effects of anlotinib in SS is mainly mediated through

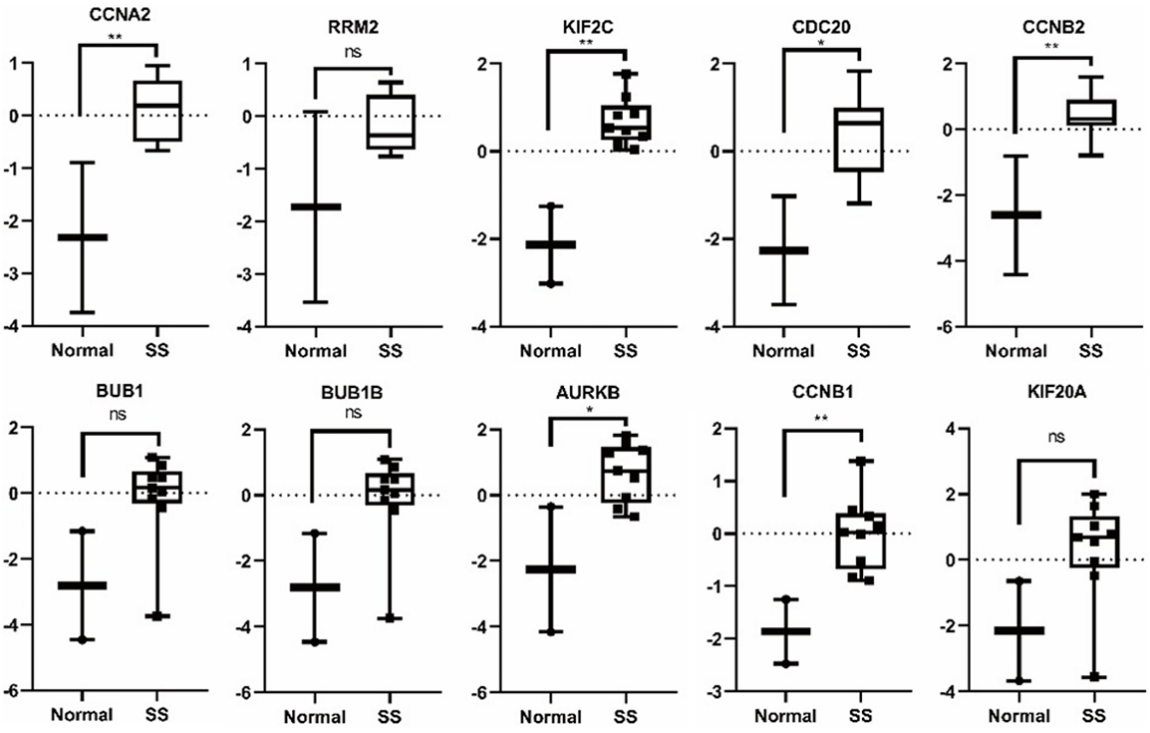

Figure 6. Expression of the top 10 hub genes verified in TCGA dataset. Analyses of the expression levels of the top 10 hub genes in synovial sarcoma tissues and normal tissues using TCGA dataset. *P<0.05 and **P<0.01, unpaired Student's t-test. TCGA, The Cancer Genome Atlas.

disrupting cell cycle progression and mitosis in the tumor cells.

Hub gene verification in SS cell lines by RT-qPCR

To further validate the effect of anlotinib on the expression of the six real hub genes (*CCNA2, KIF2C, CDC20, CCNB2, AURKB* and *CCNB1*), RT-qPCR was performed to measure the mRNA expression levels of these six real hub genes in SW982 and HS-SY-II cells treated with 2.5 μM/ml anlotinib. The results showed that after incubation with 2.5 μM/ml anlotinib for 48 h, *CCNA2, KIF2C, CDC20, CCNB2, AURKB* and *CCNB1* mRNA expression were significantly decreased in the anlotinib-treated group compared with those in the control group (**Figure 8**). These results are consistent with the microarray expression data of GSE109468, suggesting that these six hub genes function as oncogenes in the development of SS.

Discussion

In the present study, we used bioinformatics analysis to screen for the biomarkers and key pathways associated with the effects of anlotinib treatment in SS cells. By analyzing the GSE109468 dataset downloaded from the GEO database, we successfully identified 183 DEGs, of which 47 were upregulated and 136 were downregulated. Using MCC algorithm analysis combined with analysis of TCGA dataset, we finally screened six real hub genes *CCNA2, KIF2C, CDC20, CCNB2, AURKB* and *CCNB1* to be closely associated with anlotinib treatment. The results from our study will contribute to understanding the molecular mechanism underlying the effect of anlotinib treatment in SS, which will facilitate identification of the potential biomarkers and targets to improve the clinical efficacy of anlotinib in patients with SS.

According to the DAVID database, the top enriched GO and KEGG pathway enrichment analyses of the 183 DEGs were 'cell division' for BP, 'protein binding' for MF, 'nucleoplasm' for CC and 'cell cycle' for KEGG. GSEA revealed that the DEGs were mainly enriched in the E2F targets, G_2/M checkpoint and mitotic spindle. Using the STRING database and the Cytoscape software, we further constructed a PPI network of the 183 DEGs, which identified two

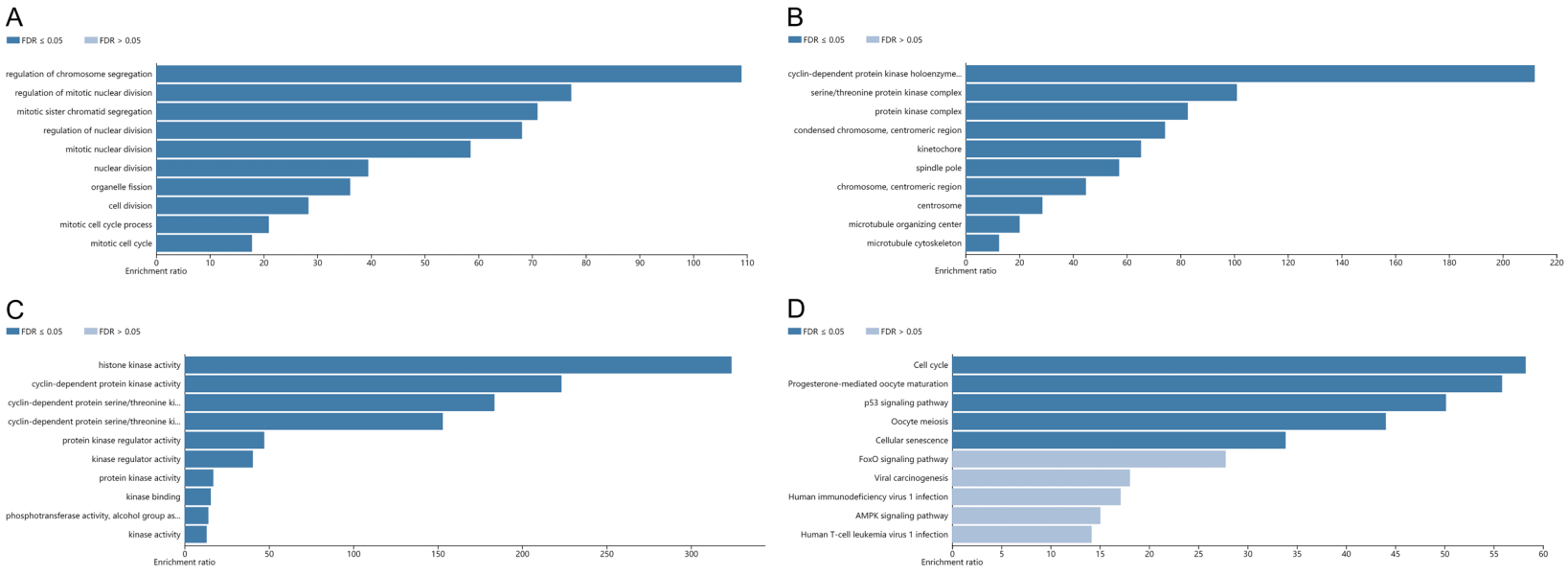

Figure 7. Significantly enriched GO and KEGG pathways of the six real hub genes using the WebGestalt database. A. Top 10 significant terms of GO Biological Process enrichment analysis. B. Top 10 significant terms of GO Cellular Component enrichment analysis. C. Top 10 significant terms of GO Molecular function enrichment analysis. D. Top 10 significant terms of KEGG pathway enrichment analysis. GO, gene ontology; KEGG, Kyoto Encyclopedia of Genes and Genomes.

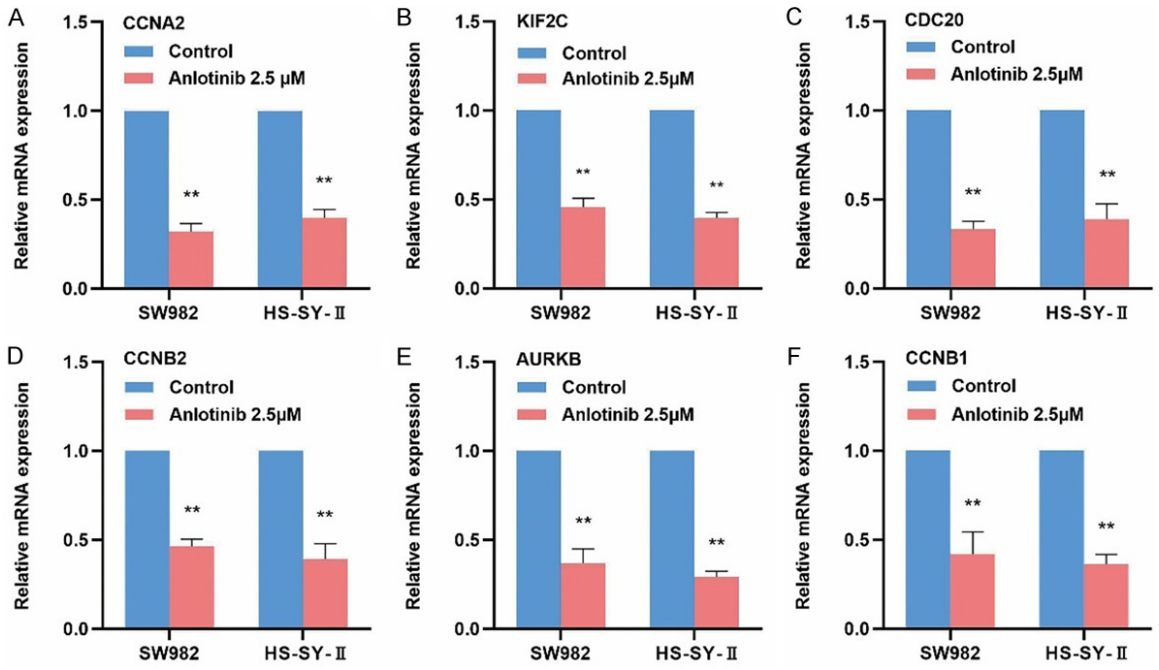

Figure 8. mRNA expression levels of the six real hub genes as validated by reverse transcription-quantitative polymerase chain reaction. The relative mRNA expression levels of the six real hub genes were significantly reduced in synovial sarcoma cells (SW982 and HS-SY-II) treated with 2.5 μM/ml anlotinib compared with those in control cells. A. *CCNA2*. B. *Kinesin family member 2C*. C. *Cell division cycle 20*. D. *CCNB2*. E. *Aurora kinase B*. F. *CCNB1*. Significant differences were reported at *P<0.05 and **P<0.01. CCN, cyclin.

modules with a score ≥5. Of the two modules, module 1 was found to be the most significant. The top enriched GO and KEGG pathways in module 1 were 'cell cycle' for BP, 'DNA replication origin binding' for MF, 'chromosome region' for CC and 'cell cycle' for KEGG. Based on module 1, the top 10 hub genes, *CCNA2, RRM2, KIF2C, CDC20, CCNB2, BUB1, BUB1B, AURKB, CCNB1* and *KIF20A*, were identified. TCGA database was then used to confirm these results, where the expression levels of *CCNA2, KIF2C, CDC20, CCNB2, AURKB* and *CCNB1* were found to be higher in SS tissues compared with those in normal tissues. These results suggest that these six real hub genes may be the closely associated with the outcomes of anlotinib treatment in patients with SS. Further analysis based on the WebGestalt database revealed that the six real hub genes were significantly associated with cell cycle and mitosis. We then validated the expression levels of these six hub genes using RT-qPCR in SS cells treated with 2.5 μM/ml anlotinib. The results showed that the mRNA levels of these six hub genes were significantly decreased after anlotinib treatment, which were consistent with the results from the microarray analysis.

CCNA2 is a highly conserved member of the cyclin family that serves a pivotal role in cell cycle progression by promoting G_1/S and G_2/M progression by interacting with cyclin dependent kinases [26, 27]. *CCNA2* has been shown to be highly expressed in various types of tumors [28], suggesting its potential roles in tumorigenesis. In addition, higher levels *CCNA2* expression have been closely associated with tamoxifen resistance in patients with breast cancer [29]. By contrast, *CCNB1* and *CCNB2* can promote the transition of cells from the G_2 into the M phase [30]. Upregulation of *CCNB1* and *CCNB2* expression has been found in a variety of human tumors, such as glioma [31], breast cancer [32, 33], as well as gastric cancer [34] and has been associated with poor prognosis [31, 32, 35]. *CDC20* is a regulator of cell cycle checkpoints and serves a key role in mitotic progression [36, 37]. It has been reported to exhibit an oncogenic role in tumorigenesis and tumor progression including prostate [38], breast cancer [39], and ovarian cancer [40]. Overexpression of *CDC20* has been documented to predict poor prognosis in various malignancies, such as pancreatic cancer and prostate cancer [41, 42], suggesting that *CDC20*

can be applied as a promising therapeutic target for cancer treatment. *KIF2C* is a member of the kinesin superfamily of microtubule motor proteins that regulates microtubule depolymerization by ensuring the correct segregation of daughter chromosomes during mitosis [43]. Elevated *KIF2C* expression has been previously reported to be associated with tumor progression and poorer survival in patients with glioma [44], breast cancer [45], lung cancer [46], colorectal cancer [47], and gastric cancer [48]. *AURKB* is an aurora kinase that can accelerate cell cycle progression from G_2 to cytokinesis by regulating chromosome segregation, arrangement and cytokinesis through binding to microtubules [49]. Previous studies have revealed that the overexpression of *AURKB* is closely associated with cancer progression and prognosis in numerous human tumors including lung cancer [50], bladder cancer [51], and osteosarcoma [52]. Taken together, our data demonstrated that almost all the six hub genes were associated with the cell cycle and mitosis. Therefore, the anti-tumor effect of anlotinib in SS may be mediated through disrupting cell cycle progression and mitosis in tumor cells.

According to the integrated bioinformatic analysis, results from our study suggest that anlotinib exerts its antitumor effect against SS mainly through the inhibition of cell cycle progression and mitosis instead of through its conventional targets, such as VEGFR, FGFR, PDGFR and c-Kit. Therefore, our results revealed a novel mechanism of anlotinib against SS.

However, the present study has some limitations that warrant consideration. The majority of the data were obtained from only one public dataset. Data pooled from multiple datasets are required to reveal the novel hub genes associated with anlotinib treatment in SS. For the verification of the expression levels of the six hub genes in SS cells, only RT-qPCR analysis was performed without using additional methods for verification, such as western blot analysis. In addition, further studies are required to explore the underlying mechanism of the six hub genes in SS both *in vivo* and *in vitro*.

Conclusions

In conclusion, using an integrated bioinformatics approach, our study identified and validated six real hub genes, namely *CCNA2, KIF2C, CDC20, CCNB2, AURKB* and *CCNB1*, to be associated with the effects of anlotinib treatment in SS. These hub genes were significantly enriched in the processes of the cell cycle and mitosis. Our results may provide insights into the molecular mechanism underlying the antitumor effects of anlotinib against SS.

Acknowledgements

This research was supported the National Natural Science Foundation of China (No. 82100787), Shandong Natural Science Foundation (No. ZR202102250120), Jinan Clinical Medicine Science and Technology Innovation Plan (No. 201907059), and the Youth Foundation of the Second Hospital of Shandong University (No. 2018YT37 and 2022YP38).

Disclosure of conflict of interest

None.

Address correspondence to: Dr. Yan Song, Department of Nephrology, The Second Hospital of Shandong University, 247# Beiyuan Street, Jinan 250033, Shandong, China. Tel: +86-17660080878; Fax: +86-0531-85875451; E-mail: songyan1581@sdu.edu.cn; Dr. Changliang Peng, Department of Spinal Surgery, The Second Hospital of Shandong University, 247# Beiyuan Street, Jinan 250033, Shandong, China. Tel: +86-18753107090; Fax: +86-0531-85875480; E-mail: pcliang@sdu.edu.cn

References

[1] Sultan I, Rodriguez-Galindo C, Saab R, Yasir S, Casanova M and Ferrari A. Comparing children and adults with synovial sarcoma in the surveillance, epidemiology, and end results program, 1983 to 2005: an analysis of 1268 patients. Cancer 2009; 115: 3537-3547.

[2] Desar IME, Fleuren EDG and van der Graaf WTA. Systemic treatment for adults with synovial sarcoma. Curr Treat Options Oncol 2018; 19: 13.

[3] Casali PG, Abecassis N, Aro HT, Bauer S, Biagini R, Bielack S, Bonvalot S, Boukovinas I, Bovee J, Brodowicz T, Broto JM, Buonadonna A, De Alava E, Dei Tos AP, Del Muro XG, Dileo P, Eriksson M, Fedenko A, Ferraresi V, Ferrari A, Ferrari S, Frezza AM, Gasperoni S, Gelderblom H, Gil T, Grignani G, Gronchi A, Haas RL, Hassan B, Hohenberger P, Issels R, Joensuu H, Jones RL, Judson I, Jutte P, Kaal S, Kasper B, Kopeckova K, Krakorova DA, Le Cesne A, Lugowska I, Merimsky O, Montemurro M, Pantaleo MA, Piana R, Picci P, Piperno-Neumann S,

Pousa AL, Reichardt P, Robinson MH, Rutkowski P, Safwat AA, Schoffski P, Sleijfer S, Stacchiotti S, Sundby Hall K, Unk M, Van Coevorden F, van der Graaf WTA, Whelan J, Wardelmann E, Zaikova O and Blay JY; ESMO Guidelines Committee and EURACAN. Soft tissue and visceral sarcomas: ESMO-EURACAN clinical practice guidelines for diagnosis, treatment and follow-up. Ann Oncol 2018; 29: iv51-iv67.

[4] von Mehren M, Kane JM, Agulnik M, Bui MM, Carr-Ascher J, Choy E, Connelly M, Dry S, Ganjoo KN, Gonzalez RJ, Holder A, Homsi J, Keedy V, Kelly CM, Kim E, Liebner D, McCarter M, McGarry SV, Mesko NW, Meyer C, Pappo AS, Parkes AM, Petersen IA, Pollack SM, Poppe M, Riedel RF, Schuetze S, Shabason J, Sicklick JK, Spraker MB, Zimel M, Hang LE, Sundar H and Bergman MA. Soft tissue sarcoma, version 2.2022, NCCN clinical practice guidelines in oncology. J Natl Compr Canc Netw 2022; 20: 815-833.

[5] de Silva MV, McMahon AD and Reid R. Prognostic factors associated with local recurrence, metastases, and tumor-related death in patients with synovial sarcoma. Am J Clin Oncol 2004; 27: 113-121.

[6] Spurrell EL, Fisher C, Thomas JM and Judson IR. Prognostic factors in advanced synovial sarcoma: an analysis of 104 patients treated at the Royal Marsden Hospital. Ann Oncol 2005; 16: 437-444.

[7] Lemmon MA and Schlessinger J. Cell signaling by receptor tyrosine kinases. Cell 2010; 141: 1117-1134.

[8] Seebacher NA, Stacy AE, Porter GM and Merlot AM. Clinical development of targeted and immune based anti-cancer therapies. J Exp Clin Cancer Res 2019; 38: 156.

[9] Kane RC, Farrell AT, Saber H, Tang S, Williams G, Jee JM, Liang C, Booth B, Chidambaram N, Morse D, Sridhara R, Garvey P, Justice R and Pazdur R. Sorafenib for the treatment of advanced renal cell carcinoma. Clin Cancer Res 2006; 12: 7271-7278.

[10] Hochmair MJ, Morabito A, Hao D, Yang CT, Soo RA, Yang JC, Gucalp R, Halmos B, Wang L, Marten A and Cufer T. Sequential afatinib and osimertinib in patients with EGFR mutation-positive non-small-cell lung cancer: updated analysis of the observational GioTag study. Future Oncol 2019; 15: 2905-2914.

[11] Llovet JM, Ricci S, Mazzaferro V, Hilgard P, Gane E, Blanc JF, de Oliveira AC, Santoro A, Raoul JL, Forner A, Schwartz M, Porta C, Zeuzem S, Bolondi L, Greten TF, Galle PR, Seitz JF, Borbath I, Haussinger D, Giannaris T, Shan M, Moscovici M, Voliotis D and Bruix J; SHARP Investigators Study Group. Sorafenib in advanced hepatocellular carcinoma. N Engl J Med 2008; 359: 378-390.

[12] Sun Y, Niu W, Du F, Du C, Li S, Wang J, Li L, Wang F, Hao Y, Li C and Chi Y. Safety, pharmacokinetics, and antitumor properties of anlotinib, an oral multi-target tyrosine kinase inhibitor, in patients with advanced refractory solid tumors. J Hematol Oncol 2016; 9: 105.

[13] Liang L, Hui K, Hu C, Wen Y, Yang S, Zhu P, Wang L, Xia Y, Qiao Y, Sun W, Fei J, Chen T, Zhao F, Yang B and Jiang X. Autophagy inhibition potentiates the anti-angiogenic property of multikinase inhibitor anlotinib through JAK2/STAT3/VEGFA signaling in non-small cell lung cancer cells. J Exp Clin Cancer Res 2019; 38: 71.

[14] Han B, Li K, Wang Q, Zhang L, Shi J, Wang Z, Cheng Y, He J, Shi Y, Zhao Y, Yu H, Zhao Y, Chen W, Luo Y, Wu L, Wang X, Pirker R, Nan K, Jin F, Dong J, Li B and Sun Y. Effect of anlotinib as a third-line or further treatment on overall survival of patients with advanced non-small cell lung cancer: the ALTER 0303 phase 3 randomized clinical trial. JAMA Oncol 2018; 4: 1569-1575.

[15] Shi J, Zhang Y, Wang J, Li J and Li Z. Anlotinib combined with chemoradiotherapy exhibits significant therapeutic efficacy in esophageal squamous cell carcinoma. Front Oncol 2020; 10: 995.

[16] Wang ZM, Zhang SL, Yang H, Zhuang RY, Guo X, Tong HX, Zhang Y, Lu WQ and Zhou YH. Efficacy and safety of anlotinib, a multikinase angiogenesis inhibitor, in combination with epirubicin in preclinical models of soft tissue sarcoma. Cancer Med 2020; 9: 3344-3352.

[17] Wang HY, Chu JF, Zhang P, Wang JQ, Yan Z, Yao SN, Yao ZH and Liu YY. Safety and efficacy of chemotherapy combined with anlotinib plus anlotinib maintenance in Chinese patients with advanced/metastatic soft tissue sarcoma. Onco Targets Ther 2020; 13: 1561-1568.

[18] Tang L, Yu W, Wang Y, Li H and Shen Z. Anlotinib inhibits synovial sarcoma by targeting GINS1: a novel downstream target oncogene in progression of synovial sarcoma. Clin Transl Oncol 2019; 21: 1624-1633.

[19] Deng W, Wang Y, Liu Z, Cheng H and Xue Y. HemI: a toolkit for illustrating heatmaps. PLoS One 2014; 9: e111988.

[20] Subramanian A, Kuehn H, Gould J, Tamayo P and Mesirov JP. GSEA-P: a desktop application for gene set enrichment analysis. Bioinformatics 2007; 23: 3251-3253.

[21] Bader GD and Hogue CW. An automated method for finding molecular complexes in large protein interaction networks. BMC Bioinformatics 2003; 4: 2.

[22] Chin CH, Chen SH, Wu HH, Ho CW, Ko MT and Lin CY. cytoHubba: identifying hub objects and sub-networks from complex interactome. BMC Syst Biol 2014; 8 Suppl 4: S11.

[23] Maere S, Heymans K and Kuiper M. BiNGO: a cytoscape plugin to assess overrepresentation of gene ontology categories in biological networks. Bioinformatics 2005; 21: 3448-3449.
[24] Wang J, Vasaikar S, Shi Z, Greer M and Zhang B. WebGestalt 2017: a more comprehensive, powerful, flexible and interactive gene set enrichment analysis toolkit. Nucleic Acids Res 2017; 45: W130-W137.
[25] Livak KJ and Schmittgen TD. Analysis of relative gene expression data using real-time quantitative PCR and the 2(-Delta Delta C(T)) method. Methods 2001; 25: 402-408.
[26] Pagano M, Pepperkok R, Verde F, Ansorge W and Draetta G. Cyclin A is required at two points in the human cell cycle. EMBO J 1992; 11: 961-971.
[27] Deng JL, Xu YH and Wang G. Identification of potential crucial genes and key pathways in breast cancer using bioinformatic analysis. Front Genet 2019; 10: 695.
[28] Kim DH, Park SE, Kim M, Ji YI, Kang MY, Jung EH, Ko E, Kim Y, Kim S, Shim YM and Park J. A functional single nucleotide polymorphism at the promoter region of cyclin A2 is associated with increased risk of colon, liver, and lung cancers. Cancer 2011; 117: 4080-4091.
[29] Gao T, Han Y, Yu L, Ao S, Li Z and Ji J. CCNA2 is a prognostic biomarker for ER+ breast cancer and tamoxifen resistance. PLoS One 2014; 9: e91771.
[30] Gavet O and Pines J. Progressive activation of CyclinB1-Cdk1 coordinates entry to mitosis. Dev Cell 2010; 18: 533-543.
[31] Wang D, Sun H, Li X, Wang G, Yan G, Ren H and Hou B. CCNB2 is a novel prognostic factor and a potential therapeutic target in low-grade glioma. Biosci Rep 2022; 42: BSR20211939.
[32] Nimeus-Malmstrom E, Koliadi A, Ahlin C, Holmqvist M, Holmberg L, Amini RM, Jirstrom K, Warnberg F, Blomqvist C, Ferno M and Fjallskog ML. Cyclin B1 is a prognostic proliferation marker with a high reproducibility in a population-based lymph node negative breast cancer cohort. Int J Cancer 2010; 127: 961-967.
[33] Sun C, Lowe S, Ma S, Bentley R, Zhou Z, Cheng C and Zhou Q. CCNB2 expression correlates with worse outcomes in breast cancer patients: a pooled analysis. Women Health 2022; 62: 655-663.
[34] Lee MH, Cho Y, Kim DH, Woo HJ, Yang JY, Kwon HJ, Yeon MJ, Park M, Kim SH, Moon C, Tharmalingam N, Kim TU and Kim JB. Menadione induces G2/M arrest in gastric cancer cells by down-regulation of CDC25C and proteasome mediated degradation of CDK1 and cyclin B1. Am J Transl Res 2016; 8: 5246-5255.
[35] Qian X, Song X, He Y, Yang Z, Sun T, Wang J, Zhu G, Xing W and You C. CCNB2 overexpression is a poor prognostic biomarker in Chinese NSCLC patients. Biomed Pharmacother 2015; 74: 222-227.
[36] Khumukcham SS, Samanthapudi VSK, Penugurti V, Kumari A, Kesavan PS, Velatooru LR, Kotla SR, Mazumder A and Manavathi B. Hematopoietic PBX-interacting protein is a substrate and an inhibitor of the APC/C-Cdc20 complex and regulates mitosis by stabilizing cyclin B1. J Biol Chem 2019; 294: 10236-10252.
[37] Wan L, Tan M, Yang J, Inuzuka H, Dai X, Wu T, Liu J, Shaik S, Chen G, Deng J, Malumbres M, Letai A, Kirschner MW, Sun Y and Wei W. APC(Cdc20) suppresses apoptosis through targeting Bim for ubiquitination and destruction. Dev Cell 2014; 29: 377-391.
[38] Mao Y, Li K, Lu L, Si-Tu J, Lu M and Gao X. Overexpression of Cdc20 in clinically localized prostate cancer: Relation to high Gleason score and biochemical recurrence after laparoscopic radical prostatectomy. Cancer Biomark 2016; 16: 351-358.
[39] Jiang J, Jedinak A and Sliva D. Ganodermanontriol (GDNT) exerts its effect on growth and invasiveness of breast cancer cells through the down-regulation of CDC20 and uPA. Biochem Biophys Res Commun 2011; 415: 325-329.
[40] Ouellet V, Guyot MC, Le Page C, Filali-Mouhim A, Lussier C, Tonin PN, Provencher DM and Mes-Masson AM. Tissue array analysis of expression microarray candidates identifies markers associated with tumor grade and outcome in serous epithelial ovarian cancer. Int J Cancer 2006; 119: 599-607.
[41] Chang DZ, Ma Y, Ji B, Liu Y, Hwu P, Abbruzzese JL, Logsdon C and Wang H. Increased CDC20 expression is associated with pancreatic ductal adenocarcinoma differentiation and progression. J Hematol Oncol 2012; 5: 15.
[42] Zhang Q, Huang H, Liu A, Li J, Liu C, Sun B, Chen L, Gao Y, Xu D and Su C. Cell division cycle 20 (CDC20) drives prostate cancer progression via stabilization of beta-catenin in cancer stem-like cells. EBioMedicine 2019; 42: 397-407.
[43] Wordeman L, Wagenbach M and von Dassow G. MCAK facilitates chromosome movement by promoting kinetochore microtubule turnover. J Cell Biol 2007; 179: 869-879.
[44] Bie L, Zhao G, Wang YP and Zhang B. Kinesin family member 2C (KIF2C/MCAK) is a novel marker for prognosis in human gliomas. Clin Neurol Neurosurg 2012; 114: 356-360.
[45] Shimo A, Tanikawa C, Nishidate T, Lin ML, Matsuda K, Park JH, Ueki T, Ohta T, Hirata K, Fukuda M, Nakamura Y and Katagiri T. Involvement of kinesin family member 2C/mitotic centromere-associated kinesin overexpression

in mammary carcinogenesis. Cancer Sci 2008; 99: 62-70.
[46] Gan H, Lin L, Hu N, Yang Y, Gao Y, Pei Y, Chen K and Sun B. KIF2C exerts an oncogenic role in nonsmall cell lung cancer and is negatively regulated by miR-325-3p. Cell Biochem Funct 2019; 37: 424-431.
[47] Gnjatic S, Cao Y, Reichelt U, Yekebas EF, Nolker C, Marx AH, Erbersdobler A, Nishikawa H, Hildebrandt Y, Bartels K, Horn C, Stahl T, Gout I, Filonenko V, Ling KL, Cerundolo V, Luetkens T, Ritter G, Friedrichs K, Leuwer R, Hegewisch-Becker S, Izbicki JR, Bokemeyer C, Old LJ and Atanackovic D. NY-CO-58/KIF2C is overexpressed in a variety of solid tumors and induces frequent T cell responses in patients with colorectal cancer. Int J Cancer 2010; 127: 381-393.
[48] Nakamura Y, Tanaka F, Haraguchi N, Mimori K, Matsumoto T, Inoue H, Yanaga K and Mori M. Clinicopathological and biological significance of mitotic centromere-associated kinesin overexpression in human gastric cancer. Br J Cancer 2007; 97: 543-549.
[49] Goldenson B and Crispino JD. The aurora kinases in cell cycle and leukemia. Oncogene 2015; 34: 537-545.
[50] Takeshita M, Koga T, Takayama K, Ijichi K, Yano T, Maehara Y, Nakanishi Y and Sueishi K. Aurora-B overexpression is correlated with aneuploidy and poor prognosis in non-small cell lung cancer. Lung Cancer 2013; 80: 85-90.
[51] Mobley A, Zhang S, Bondaruk J, Wang Y, Majewski T, Caraway NP, Huang L, Shoshan E, Velazquez-Torres G, Nitti G, Lee S, Lee JG, Fuentes-Mattei E, Willis D, Zhang L, Guo CC, Yao H, Baggerly K, Lotan Y, Lerner SP, Dinney C, McConkey D, Bar-Eli M and Czerniak B. Aurora kinase A is a biomarker for bladder cancer detection and contributes to its aggressive behavior. Sci Rep 2017; 7: 40714.
[52] Zhao Z, Jin G, Yao K, Liu K, Liu F, Chen H, Wang K, Gorja DR, Reddy K, Bode AM, Guo Z and Dong Z. Aurora B kinase as a novel molecular target for inhibition the growth of osteosarcoma. Mol Carcinog 2019; 58: 1056-1067.

Table S1. The primers used for qRT-PCR

Gene	Primers	
CCNA2	forward	5'-CGCTGGCGGTACTGAAGTC-3'
	reverse	5'-GAGGAACGGTGACATGCTCAT-3'
KIF2C	forward	5'-CAGAACTCTTACAGCTTCTTCCC-3'
	reverse	5′-CAGTGGACATGCGAGTGGA-3'
CDC20	forward	5'-GACCACTCCTAGCAAACCTGG-3'
	reverse	5'-GGGCGTCTGGCTGTTTTCA-3'
CCNB2	forward	5'-CCGACGGTGTCCAGTGATTT-3'
	reverse	5'-TGTTGTTTTGGTGGGTTGAACT-3'
AURKB	forward	5'-CAGTGGGACACCCGACATC-3'
	reverse	5'-GTACACGTTTCCAAACTTGCC-3'
CCNB1	forward	5'-AATAAGGCGAAGATCAACATGGC-3'
	reverse	5'-TTTGTTACCAATGTCCCCAAGAG-3'
β-actin	forward	5'-CATGTACGTTGCTATCCAGGC-3'
	reverse	5'-CTCCTTAATGTCACGCACGAT-3'

Table S2. List of GO terms of BP of the six hub genes analyzed via the WebGestalt

GeneSet	Description	Enrichment Ratio	FDR	Genes
GO:0051983	regulation of chromosome segregation	108.97	2.23E-05	*KIF2C; CDC20; AURKB; CCNB1*
GO:0007088	regulation of mitotic nuclear division	77.29	1.86E-06	*CCNA2; CDC20; CCNB2; AURKB; CCNB1*
GO:0000070	mitotic sister chromatid segregation	71.01	8.52E-05	*KIF2C; CDC20; AURKB; CCNB1*
GO:0051783	regulation of nuclear division	68.11	2.82E-06	*CCNA2; CDC20; CCNB2; AURKB; CCNB1*
GO:0140014	mitotic nuclear division	58.54	2.14E-07	*CCNA2; KIF2C; CDC20; CCNB2; AURKB; CCNB1*
GO:0000280	nuclear division	39.50	1.16E-06	*CCNA2; KIF2C; CDC20; CCNB2; AURKB; CCNB1*
GO:0048285	organelle fission	36.12	1.32E-06	*CCNA2; KIF2C; CDC20; CCNB2; AURKB; CCNB1*
GO:0051301	cell division	28.37	2.83E-06	*CCNA2; KIF2C; CDC20; CCNB2; AURKB; CCNB1*
GO:1903047	mitotic cell cycle process	20.98	1.50E-05	*CCNA2; KIF2C; CDC20; CCNB2; AURKB; CCNB1*
GO:0000278	mitotic cell cycle	17.85	3.08E-05	*CCNA2; KIF2C; CDC20; CCNB2; AURKB; CCNB1*

Table S3. List of GO terms of CC of the six hub genes analyzed via WebGestalt

GeneSet	Description	Enrichment Ratio	FDR	Genes
GO:0000307	cyclin-dependent protein kinase holoenzyme complex	211.90	1.42E-04	*CCNA2; CCNB2; CCNB1*
GO:1902554	serine/threonine protein kinase complex	101.02	6.79E-04	*CCNA2; CCNB2; CCNB1*
GO:1902911	protein kinase complex	82.74	9.93E-04	*CCNA2; CCNB2; CCNB1*
GO:0000779	condensed chromosome, centromeric region	74.26	0.001146	*KIF2C; AURKB; CCNB1*
GO:0000776	kinetochore	65.32	0.001264	*KIF2C; AURKB; CCNB1*
GO:0000922	spindle pole	57.16	0.001678	*CDC20; AURKB; CCNB1*
GO:0000775	chromosome, centromeric region	44.78	0.002915	*KIF2C; AURKB; CCNB1*
GO:0005813	centrosome	28.62	1.41E-04	*KIF2C; CDC20; CCNB2; AURKB; CCNB1*
GO:0005815	microtubule organizing center	20.11	2.73E-04	*KIF2C; CDC20; CCNB2; AURKB; CCNB1*
GO:0015630	microtubule cytoskeleton	12.46	0.00126	*KIF2C; CDC20; CCNB2; AURKB; CCNB1*

Table S4. List of GO terms of MF of the six hub genes analyzed via WebGestalt

GeneSet	Description	Enrichment Ratio	FDR	Genes
GO:0035173	histone kinase activity	324.02	0.009296	*AURKB; CCNB1*
GO:0097472	cyclin-dependent protein kinase activity	223.31	3.51E-04	*CCNA2; CCNB2; CCNB1*
GO:0016538	cyclin-dependent protein serine/threonine kinase regulator activity	183.61	3.51E-04	*CCNA2; CCNB2; CCNB1*
GO:0004693	cyclin-dependent protein serine/threonine kinase activity	153.01	0.01431	*CCNB2; CCNB1*
GO:0019887	protein kinase regulator activity	47.21	0.010669	*CCNA2; CCNB2; CCNB1*
GO:0019207	kinase regulator activity	40.50	0.01125	*CCNA2; CCNB2; CCNB1*
GO:0004672	protein kinase activity	17.05	0.01125	*CCNA2; CCNB2; AURKB; CCNB1*
GO:0019900	kinase binding	15.54	0.012572	*CCNA2; CCNB2; AURKB; CCNB1*
GO:0016773	phosphotransferase activity, alcohol group as acceptor	14.12	0.01431	*CCNA2; CCNB2; AURKB; CCNB1*
GO:0016301	kinase activity	13.08	0.017296	*CCNA2; CCNB2; AURKB; CCNB1*

Table S5. List of enriched KEGG pathways of the six hub genes analyzed via WebGestalt

GeneSet	Description	Enrichment Ratio	FDR	Genes
hsa04110	Cell cycle	58.24	2.70E-05	*CCNA2; CDC20; CCNB2; CCNB1*
hsa04914	Progesterone-mediated oocyte maturation	55.84	0.001517	*CCNA2; CCNB2; CCNB1*
hsa04115	p53 signaling pathway	50.15	0.037853	*CCNB2; CCNB1*
hsa04114	Oocyte meiosis	44.04	0.00207	*CDC20; CCNB2; CCNB1*
hsa04218	Cellular senescence	33.85	0.003423	*CCNA2; CCNB2; CCNB1*
hsa04068	FoxO signaling pathway	27.78	0.102371	*CCNB2; CCNB1*
hsa05203	Viral carcinogenesis	18.06	0.199811	*CCNA2; CDC20*
hsa05170	Human immunodeficiency virus 1 infection	17.11	0.199811	*CCNB2; CCNB1*
hsa04152	AMPK signaling pathway	15.05	1	*CCNA2*
hsa05166	Human T-cell leukemia virus 1 infection	14.16	0.25748	*CDC20; CCNB2*